

Superconducting gap and enhanced superconductivity by cleaving process in KV_3Sb_5

Wei Chen,^{1,*} Lichen Ji,^{1,*} Xinyu Zhou,^{1,*} Hongxiu Liu,² Fanqi Meng,² Zichun Zhang,¹ Yaowu Liu,¹ Xiaopeng Hu,¹ Qinghua Zhang,² Youguo Shi,² Lin Gu,³ Xi Chen,^{1,4,5} Qi-Kun Xue,^{1,4,5} and Shuai-Hua Ji^{1,4,5,†}

¹State Key Laboratory of Low-Dimensional Quantum Physics, Department of Physics, Tsinghua University, Beijing 100084, China

²Beijing National Laboratory for Condensed Matter Physics, Institute of Physics, Chinese Academy of Sciences, Beijing 100190, China

³School of Materials Science and Engineering, Tsinghua University, Beijing 100084, China

⁴Frontier Science Center for Quantum Information, Beijing 100084, China

⁵Collaborative Innovation Center of Quantum Matter, Beijing 100084, China



(Received 25 December 2023; accepted 17 June 2024; published 9 July 2024)

Kagome superconductors AV_3Sb_5 ($A = K, Rb, Cs$) have attracted great attention recently due to the topological electronic bands and rich many-body states. Here, we report the unusual superconducting gap of about 0.10 meV of KV_3Sb_5 , which cannot be fitted by BCS theory, measured by a dilution refrigerator scanning tunneling microscope. Uniform superconducting gaps on a potassium-terminated surface have been revealed by spatially resolved scanning tunneling spectra. Temperature-dependent tunneling spectra unveil that the superconducting transition temperature is about 0.73 K on a cleaved surface. Due to the desorption of potassium, it is slightly lower than the bulk superconducting transition temperature of 0.92 K determined by transport measurement. In addition, our electronic transport measurement of thin flakes shows an enhanced superconducting transition onset temperature up to 2.15 K, which is possibly attributed to the strain effect caused by their underlying cleaving tapes. Our work sheds light on understanding the unusual superconducting state of a vanadium-based kagome superconductor.

DOI: [10.1103/PhysRevMaterials.8.074601](https://doi.org/10.1103/PhysRevMaterials.8.074601)

I. INTRODUCTION

Crystal structure with kagome lattice hosts many interesting electronic states, such as topological Dirac fermions, flat bands with strong correlation or magnetism, and van Hove singularities [1–4]. Those interesting features of the electronic band of AV_3Sb_5 , including topological nontrivial bands, have been studied by density function calculations (density-functional theory) and angle-resolved photoemission spectroscopy [1,3,5–7].

In addition to the unusual electronic band structures, charge density waves (CDWs) are discovered in these AV_3Sb_5 kagome metals, indicating the existence of a correlation effect [8–11]. The CDW transition temperatures of AV_3Sb_5 kagome metals are as high as 78 K for KV_3Sb_5 , 94 K for CsV_3Sb_5 , and 103 K for RbV_3Sb_5 [12,13]. These first-order phase transition temperatures have been precisely determined by electronic transport and nuclear magnetic resonance. The momentum-resolved gap structures of the CDW phase of kagome metals are crucial to understanding the underlying mechanism of these many-body correlated electronic states. The van Hove filling near the Fermi level has been suggested to play a role in the unconventional CDW in kagome metals in several studies [14,15], whereas another report indicates the electron-phonon coupling induced structure transition mainly drives the CDW in KV_3Sb_5 [5].

Superconductivity and related exotic states emerge in AV_3Sb_5 kagome metals at lower temperature. The coexistence of the superconductivity and the band topology or CDW leads to many interesting physics in AV_3Sb_5 kagome metals [16–18], such as topological superconductivity. Recently, the evidence of this topological nontrivial superconductivity of CsV_3Sb_5 has been revealed, where a robust zero bias conductance (ZBC) peak without splitting in a large distance from the vortex core has been observed on a $Cs\ 2 \times 2$ surface [16]. The intertwining of CDW and superconductivity is a common behavior of all AV_3Sb_5 materials, in which the double-dome behavior under pressure was widely explored [19]. More intriguingly, pair density wave states are evidenced in CsV_3Sb_5 by dI/dV maps at an energy level near the superconducting gap edge [17]. In the nanopatterned ring devices of CsV_3Sb_5 , even the exotic charge- $4e$ and charge- $6e$ superconducting states have been reported [20].

A sharp superconducting transition at 0.93 K of bulk KV_3Sb_5 , which is relatively lower than CsV_3Sb_5 , is determined in a pioneering transport measurement [21]. However, so far, the superconducting gap of KV_3Sb_5 has not been studied by tunneling experiments due to the lower superconducting transition temperature. Here, we employ dilution refrigerator scanning tunneling microscopy (STM) to investigate the superconducting gap structure. We find that it cannot be well fitted by BCS theory with an s -wave single-gap model, but a p -wave or d -wave model shows a better fit result which indicates possible unusual superconductivity. Furthermore, we find that the superconducting transition onset temperature of KV_3Sb_5 is significantly increased by a tape cleaving pro-

*These authors contributed equally to this work.

†Contact author: shji@mail.tsinghua.edu.cn

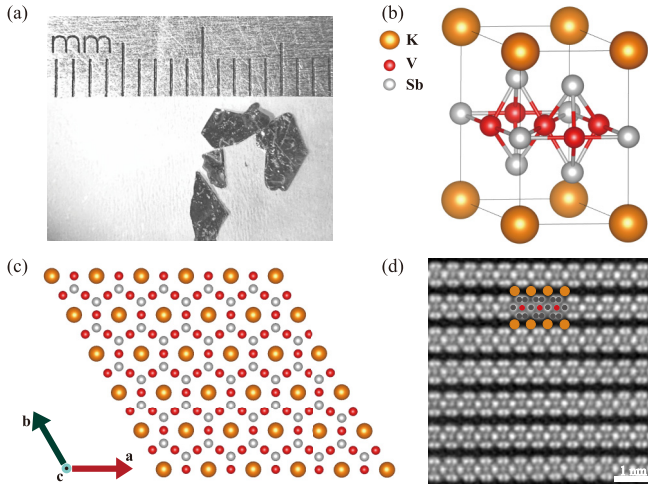


FIG. 1. Crystal structure of KV_3Sb_5 . (a) Optical image of our synthesized KV_3Sb_5 single crystal. (b) One unit cell of KV_3Sb_5 crystal. The red, yellow, and gray balls represent V, K, and Sb atoms, respectively. (c) The top view of the atomic structure along the c -axis of KV_3Sb_5 . (d) A high-angle annular dark-field cross-sectional STEM image of KV_3Sb_5 along the $[110]$ direction.

cess up to 2.1 K, which may be attributed to the strain effect imposed by the tape under the cleaved KV_3Sb_5 flakes.

II. EXPERIMENT

Single crystals of KV_3Sb_5 with a lateral size up to 5 mm [Fig. 1(a)], which are used in our experiments, were grown by the flux method from KSb_2 alloy and Sb as flux. A stoichiometric amount of K, V, Sb, and KSb_2 precursor were sealed in a Ta crucible with a mole ratio of 1:3:14:10 and then finally sealed in a highly evacuated quartz ampoule. The ampoule was heated up to 1273 K, kept at 1273 K for 20 hours, and then cooled down to 773 K at a rate of 2 K/h. Shiny single crystals were separated from the flux by centrifuging.

Samples characterized by STM and scanning tunneling spectroscopy (STS) were cleaved in an ultra-high vacuum environment at room temperature (samples are glued on holders by standard silver-filled epoxy, and no strain effect is expected on STM samples). Then they were immediately transferred into an ultra-low-temperature STM with a base pressure of 1×10^{-10} Torr. With the help of a dilution refrigerator, the temperature of the STM head can reach 60 mK and the electronic temperature of samples is around 230 mK [22], which is sufficiently lower than the superconducting transition temperature of bulk KV_3Sb_5 . The dI/dV spectra are measured by standard lock-in technique with a modulation frequency of 991 Hz, and each curve is obtained by averaging six measurements. A smooth process has been adapted for reducing noise of spectra but without removing intrinsic features. In addition, the atomic structure of our samples is characterized by *ex situ* scanning transmission electron microscopy (STEM).

Besides STM/STS measurements which provide information on local superconducting gap of KV_3Sb_5 , we conducted electrical transport measurements on cleaved single crystals of KV_3Sb_5 down to the lowest temperature of 500 mK and with a perpendicular magnetic field up to 9 T. Considering

that the resistance of bulk crystals is quite small and lower than the resolution of our transport measurement system, we used sticky tape to cleave the single crystals to thinner flakes and then stuck them together with the sticky tape to the sample holder. After the cleaving process, some parts of the KV_3Sb_5 flakes on sticky tape are bent and show a curved surface (see Fig. S1 in the Supplemental Material [23]). The thickness of these flakes determined by scanning electron microscopy is around few micrometers (see Fig. S2 in the Supplemental Material [23]). The measuring current in our four-terminal transport measurement was set to 100 μ A.

III. RESULTS

A single unit cell of layered kagome superconductor KV_3Sb_5 exhibits a hexagonal crystal structure as shown in Fig. 1(b), which is composed of an alternately stacked K atoms plane and V-Sb plane. In the middle of this V-Sb plane, a kagome lattice of V atoms intertwines with hexagonal structure of Sb atoms, as shown in Fig. 1(c), which separates the triangular structure of K atoms. Figure 1(d) shows a high-angle annular dark-field STEM image of the KV_3Sb_5 crystal along the $[110]$ direction. In dark-field mode, the hexagonal lattice of Sb atoms and V atoms can be clearly seen, whereas the rows of potassium atoms are rather weak. The uniform and orderly arrangement of atoms in the STEM image shows the high quality of our synthesized single-crystal samples. The lattice constant of our samples is determined from the STEM image: $a = b = 5.35 \pm 0.06$ Å and $c = 8.62 \pm 0.02$ Å, which are consistent with a previous report [24].

The topography and electronic states of freshly cleaved surface of KV_3Sb_5 single crystal have been characterized by a low-temperature STM/STS measurement. As shown in Fig. 2(a), the cleaved surface presents neither kagome lattice nor hexagonal lattice structure. The cleaved surface is relatively flat with a roughness of 0.5 nm but shows disordered stripes of several nanometers. The disordered topography is related to the desorption of potassium atoms from the cleaved surface. At room temperature, the surface potassium atoms are unstable and the partial desorption of potassium atoms happens after cleaving. When the sample is transferred into the low-temperature STM head, the cleaved plane remains disordered in topography. At liquid helium temperature, the spectroscopic measurement shows finite density of states around the Fermi level, as shown in Fig. 2(b). Around the Fermi level, it shows a 20-meV electronic gap, which is most probably caused by the CDW of kagome lattice surface of the V-Sb slab and consistent with a previous report [12]. At ultra-low temperature around 60 mK, a small superconducting gap of about 0.10 meV can be observed. The superconducting coherence peaks are not sharp, and the superconducting gap cannot be well fitted by the BCS model, as shown in Fig. 2(c). During the fitting process, we used the Dynes formula for the excitation spectrum of superconductors [25], and a thermal broadening effect is considered by adding the Fermi distribution function. In Fig. 2(c), the red curve is the fit from a single gap s -wave superconductor model, yet the black and green curves from the p -wave and d -wave models show a better fit result. This indicates that the KV_3Sb_5 may have unusual superconducting properties [26]. Although the

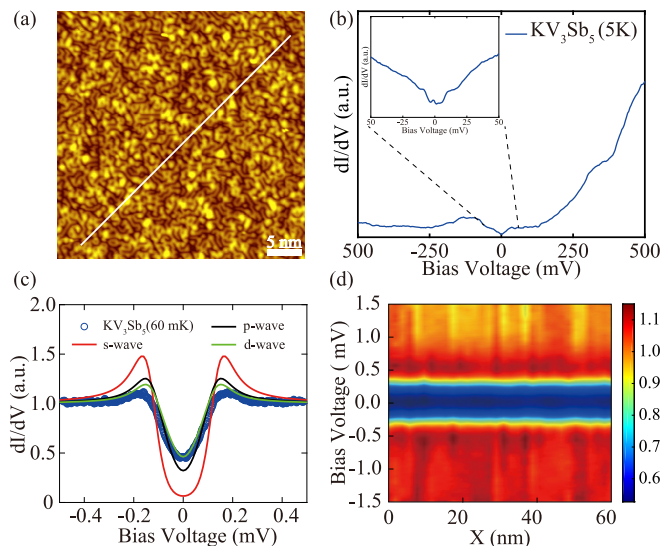


FIG. 2. Topography and tunneling spectra of KV_3Sb_5 . (a) Topography of a cleaved KV_3Sb_5 single crystal with the exposed potassium atoms ($V_s = 2.0$ V, $I_t = 20$ pA, 50×50 nm). (b) The dI/dV spectrum on the cleaved surface ($V_s = 0.5$ V, $I_t = 100$ pA). Inset: dI/dV spectrum near the Fermi level with a smaller bias range ($V_s = 0.05$ V, $I_t = 100$ pA). (c) The superconducting gap spectrum of KV_3Sb_5 . The blue line represents experimental data. The red line represents the s -wave model (superconducting parameter $\Delta = 0.13$ meV, quasiparticle lifetime $\Gamma = 0.005$ meV). The black line represents the p -wave model [$\Delta(\theta) = 0.13\cos(\theta)$ meV, $\Gamma = 0.005$ meV]. The green line represents the d -wave model [$\Delta(\theta) = 0.13\cos^2(\theta)$ meV, $\Gamma = 0.005$ meV]. (d) Spatially resolved dI/dV spectra (evenly distributed 32 curves) along the white line (60 nm) in (a), which shows a spatially uniform superconducting gap. The average spectrum magnitude of each curve is normalized to 1. At each measuring position, the STM tip is stabilized for 0.5 s before the feedback loop of the STM is closed for STS measurement.

morphology of the cleaved surface is rather disordered, the superconducting gap is extremely uniform across a 60-nm length scale as shown in Fig. 2(d), which indicates the robust superconductivity of KV_3Sb_5 against disorder. Considering that the potassium layer is a charge reservoir layer and the large coherence length of about 200 nm [27], which is much larger than the disorder length scale of a few nanometers shown in Fig. 2(a), the effect of the disorder of the potassium layer on the shape of the superconducting gap should be weak.

Temperature-dependent dI/dV spectra reveal the superconducting phase transition of KV_3Sb_5 . As shown in Fig. 3(a), the superconducting gap of KV_3Sb_5 gradually shrinks as the temperature increases and fully closes above 0.71 K. The temperature-dependent ZBC is shown in Fig. 3(b). From the linear fit of ZBC from 0.25 to 0.71 K, a superconducting transition temperature of 0.73 K of the cleaved surface is derived, which is lower than the previous report [21]. We should note that what we measured here is the surface superconducting transition temperature of an exposed potassium plane. Due to the desorption of potassium of the cleaved surface, it is reasonable that the surface superconducting transition temperature is slightly lower than the bulk.

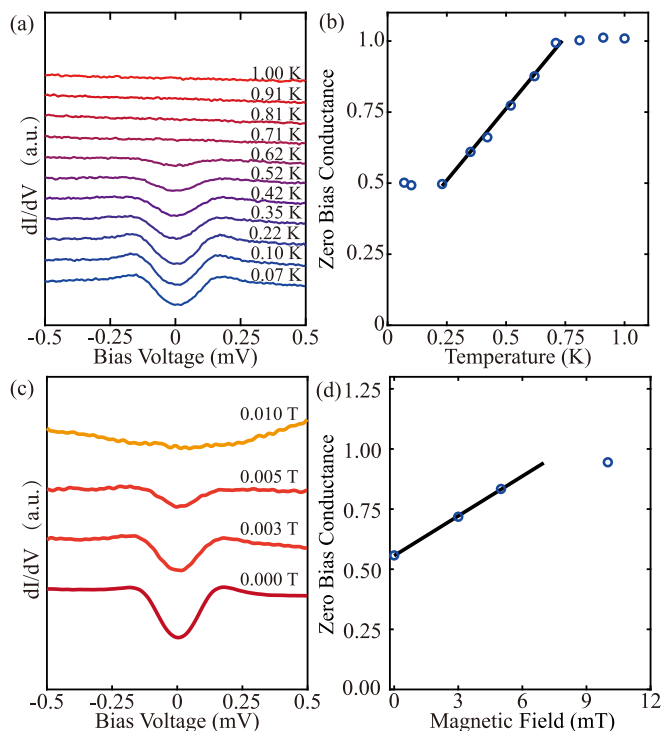


FIG. 3. Temperature- and magnetic-field-dependent spectra. (a) Tunneling spectra of KV_3Sb_5 at different temperatures from 0.07 to 1.00 K ($V_s = 0.5$ mV, $I_t = 100$ pA). (b) Temperature-dependent ZBC of superconducting spectra (blue scatters) and linear fit (black line) from 0.22 to 0.73 K. The extracted transition temperature is around 0.73 K. (c) Tunneling spectra of KV_3Sb_5 under out-of-plane magnetic fields from 0 to 0.010 T ($V_s = 0.5$ mV, $I_t = 100$ pA). (d) Magnetic-field-dependent ZBC of superconducting spectra (blue scatters) and linear fit (black line) from 0 to 0.007 T. The extracted upper critical field is around 0.007 T.

The response of the superconducting gap spectrum under magnetic fields is also measured. As shown in Fig. 3(c), an out-of-plane magnetic field of less than 0.01 T can destroy the superconductivity of KV_3Sb_5 . Due to the extremely low upper critical field of KV_3Sb_5 and limited scanning size of our STM, it is hard to find a vortex on KV_3Sb_5 in our current experiment. From the linear fit of magnetic-field-dependent ZBC of the superconducting gaps, the extracted upper critical field is around 0.007 T as shown in Fig. 3(d), which indicates that the superconductivity of KV_3Sb_5 is easily suppressed by external magnetic fields.

The electronic transport measurement shown in Fig. 4 reveals the clear superconducting phase transition in cleaved KV_3Sb_5 thin flakes (about 2 μm thick). The temperature- and field-dependent in-plane resistances are shown in Fig. 4. In the resistance-temperature (R-T) curves in Fig. 4(a), the in-plane resistance shows an almost linear relationship with temperature from 40 to 200 K, showing a well-defined metallic behavior, and drops to zero at about $T_{c0} = 0.92$ K as indicated by the downward arrow in Fig. 4(a), which is consistent with previous work [21]. The absence of the CDW signal may be attributed to the inhomogeneity of our cleaved sample. From 2.15 K [marked by an upward arrow in Fig. 4(a)] to 1 K, it shows an unusual continuous decrease, deviating

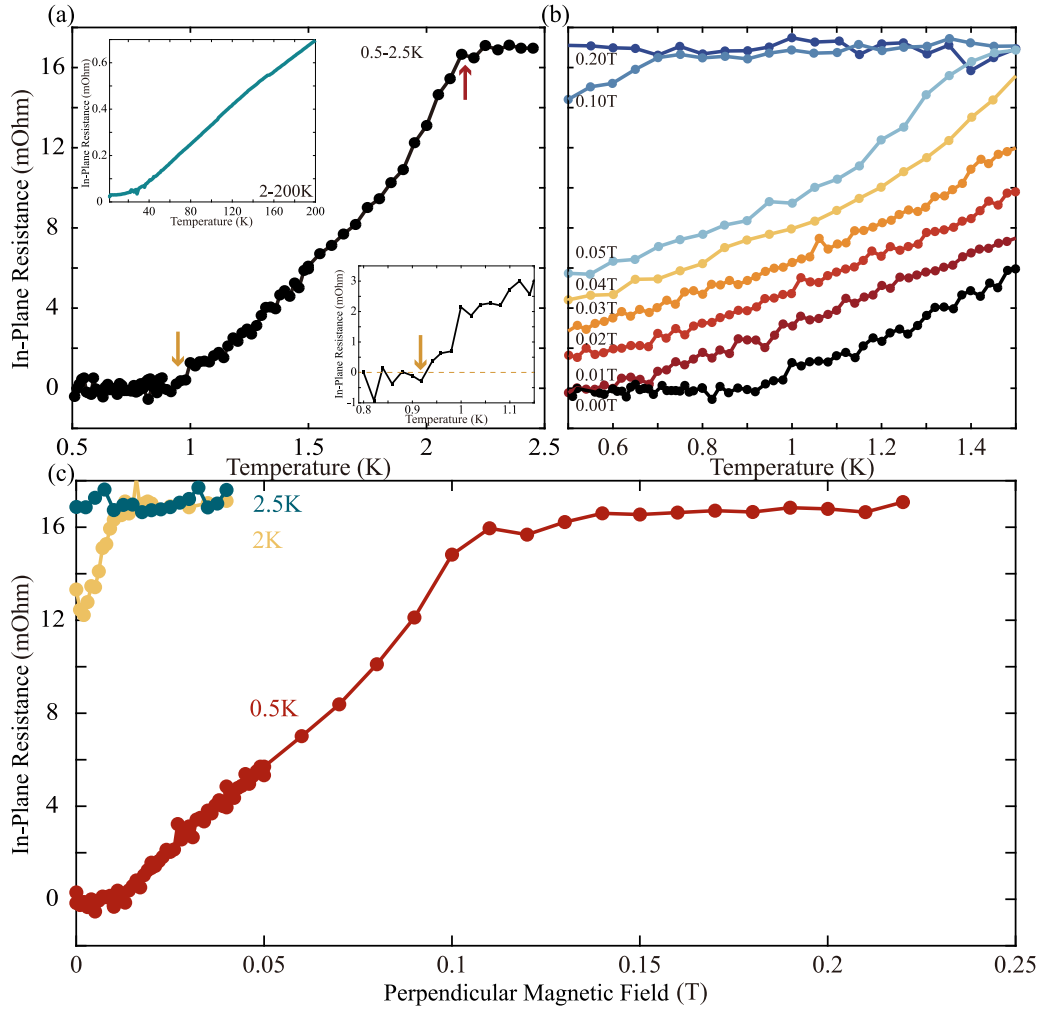


FIG. 4. Electrical transport measurement. (a) Temperature-dependent in-plane resistance of cleaved KV₃Sb₅ from 0.5 to 2 K (the red arrow indicates the superconductivity onset temperature, and the yellow arrow marks the zero resistance temperature) and from 2 to 200 K (upper insert). The magnified R-T curve from 1.1 to 0.8 K is shown in the lower insert (the yellow arrow indicates the zero resistance temperature). (b) R-T curves from 0.5 to 1.5 K at the magnetic field of magnitudes from 0 to 0.2 T. (c) Field-dependent resistance curve at 0.5, 2, and 2.5 K.

from the expected metallic R-T curve, which will be discussed later. To confirm the superconducting behavior, we measured R-T curves under different perpendicular magnetic fields [Fig. 4(b)]. From 1.5 to 0.5 K, the resistance decreases continuously and the zero resistance behavior in the R-T curve vanishes when the magnetic field of 0.02 T or higher magnitude is applied. Finally, when the magnetic field reaches 0.2 T, the resistance remains almost constant from 1.5 to 0.5 K.

The resistance-field (R-H) curves at 0.5 K shown in Fig. 4(c) also demonstrate how the magnetic field destroys the superconductivity. The resistance becomes a finite value as the magnetic field increases to 0.014 T, and it increases with magnetic fields and finally saturates at around 0.15 T. The R-H curves at 2.0 and 2.5 K are also shown in Fig. 4(c). Interestingly, compared with the resistance of the normal state at 2.5 K (green curve) which remains almost constant with the external magnetic field, the in-plane resistance at 2 K shows a clear drop around 0.01 T. Combined with the unusual drop behavior of the resistance around 2 K in Fig. 4(a), we believe that the resistance decrease at 2.15 K indicates the

onset of a superconducting state in part of our sample. Since the resistance shows a continuous drop from 2.15 to 1 K, we expect that the superconductivity of our sample is highly inhomogeneous and the superconducting transition temperature of different parts varies from 2.15 to 1 K. Comparing to the bulk, the enhanced superconductivity may arise from the sticky tape between the sample and sample holder, which might add stress on part of the sample and cause the superconductivity enhancement. This is consistent with previous work showing that the small pressure, such as 0.5 GPa, can increase the transition temperature in a bulk KV₃Sb₅ sample up to 3.1 K [28]. In our sample, we expect that the largest effective compressive pressure is about 0.25 GPa and the corresponding lattice distortion is around 0.25% [29].

IV. CONCLUSIONS

To explore the superconductivity of kagome metal KV₃Sb₅, we conducted both local superconducting gap and electrical transport measurements on cleaved KV₃Sb₅ thin

flakes. The unusual superconducting gap, which cannot be fitted by BCS theory, on a cleaved surface of KV_3Sb_5 is revealed by STS at 60 mK. The temperature-dependent dI/dV spectra show that the superconducting gap closing temperature is around 0.73 K, which is slightly lower than the bulk transition temperature determined by transport measurements possibly due to the desorption of a potassium atom on a cleaved surface. In addition, the upper critical magnetic field determined by the gap spectra is around 7 mT. Furthermore, in the electronic transport measurements, we find a transition from finite to zero resistance around 0.92 K, which corresponds to the bulk superconducting transition temperature T_{c0} . Surprisingly, we also find that there is another resistance drop at around 2.15 K, which is significantly higher than T_{c0} . We inferred that this enhancement of superconductivity might arise from the strain effect induced by the bottom sticky tape. Our systematic

studies from both macroscopic and microscopic approaches further the understanding of the superconductivity of kagome metals.

ACKNOWLEDGMENTS

We thank Y. J. Yan for preparation of the TEM sample, as well as X. B. Ma and K. L. Jiang for scanning electron microscopy measurement. This work was supported by the Ministry of Science and Technology of China (Grants No. 2021YFE0107900 and No. 2018YFA0305603), the National Natural Science Foundation of China (Grants No. 12074211, No. 12141403, No. 52388201, No. U2032204, No. 52250402, and No. 52072400), and the Strategic Priority Research Program of the Chinese Academy of Sciences (Grant No. XDB33010000).

-
- [1] J.-X. Yin, B. Lian, and M. Z. Hasan, Topological kagome magnets and superconductors, *Nature (London)* **612**, 647 (2022).
- [2] K. Jiang, T. Wu, J.-X. Yin, Z. Wang, M. Z. Hasan, S. D. Wilson, X. Chen, and J. Hu, Kagome superconductors AV_3Sb_5 ($A=K, Rb, Cs$), *Natl. Sci. Rev.* **10**, nwac199 (2023).
- [3] B. R. Ortiz, S. M. L. Teicher, Y. Hu, J. L. Zuo, P. M. Sarte, E. C. Schueller, A. M. M. Abeykoon, M. J. Krogstad, S. Rosenkranz, R. Osborn, R. Seshadri, L. Balents, J. He, and S. D. Wilson, CsV_3Sb_5 : A Z_2 topological kagome metal with a superconducting ground state, *Phys. Rev. Lett.* **125**, 247002 (2020).
- [4] V. Scagnoli, D. D. Khalyavin, and S. W. Lovesey, Hidden magnetic order on a kagome lattice for KV_3Sb_5 , *Phys. Rev. B* **106**, 064419 (2022).
- [5] H. Luo, Q. Gao, H. Liu, Y. Gu, D. Wu, C. Yi, J. Jia, S. Wu, X. Luo, Y. Xu, L. Zhao, Q. Wang, H. Mao, G. Liu, Z. Zhu, Y. Shi, K. Jiang, J. Hu, Z. Xu, and X. J. Zhou, Electronic nature of charge density wave and electron-phonon coupling in kagome superconductor KV_3Sb_5 , *Nat. Commun.* **13**, 273 (2022).
- [6] H. Li, T. T. Zhang, T. Yilmaz, Y. Y. Pai, C. E. Marvinney, A. Said, Q. W. Yin, C. S. Gong, Z. J. Tu, E. Vescovo, C. S. Nelson, R. G. Moore, S. Murakami, H. C. Lei, H. N. Lee, B. J. Lawrie, and H. Miao, Observation of unconventional charge density wave without acoustic phonon anomaly in kagome superconductors AV_3Sb_5 ($A = Rb, Cs$), *Phys. Rev. X* **11**, 031050 (2021).
- [7] Z. Liu, N. Zhao, Q. Yin, C. Gong, Z. Tu, M. Li, W. Song, Z. Liu, D. Shen, Y. Huang, K. Liu, H. Lei, and S. Wang, Charge-density-wave-induced bands renormalization and energy gaps in a kagome superconductor RbV_3Sb_5 , *Phys. Rev. X* **11**, 041010 (2021).
- [8] H. Zhao, H. Li, B. R. Ortiz, S. M. Teicher, T. Park, M. Ye, Z. Wang, L. Balents, S. D. Wilson, and I. Zeljkovic, Cascade of correlated electron states in the kagome superconductor CsV_3Sb_5 , *Nature (London)* **599**, 216 (2021).
- [9] L. Zheng, Z. Wu, Y. Yang, L. Nie, M. Shan, K. Sun, D. Song, F. Yu, J. Li, D. Zhao, S. Li, B. Kang, Y. Zhou, K. Liu, Z. Xiang, J. Ying, Z. Wang, T. Wu, and X. Chen, Emergent charge order in pressurized kagome superconductor CsV_3Sb_5 , *Nature (London)* **611**, 682 (2022).
- [10] C. Mielke III, D. Das, J.-X. Yin, H. Liu, R. Gupta, Y.-X. Jiang, M. Medarde, X. Wu, H. C. Lei, J. Chang, P. Dai, Q. Si, H. Miao, R. Thomale, T. Neupert, Y. Shi, R. Khasanov, M. Z. Hasan, H. Luetkens, and Z. Guguchia, Time-reversal symmetry-breaking charge order in a kagome superconductor, *Nature (London)* **602**, 245 (2022).
- [11] L. Nie *et al.*, Charge-density-wave-driven electronic nematicity in a kagome superconductor, *Nature (London)* **604**, 59 (2022).
- [12] Y.-X. Jiang *et al.*, Unconventional chiral charge order in kagome superconductor KV_3Sb_5 , *Nat. Mater.* **20**, 1353 (2021).
- [13] H. Li, H. Zhao, B. R. Ortiz, T. Park, M. Ye, L. Balents, Z. Wang, S. D. Wilson, and I. Zeljkovic, Rotation symmetry breaking in the normal state of a kagome superconductor KV_3Sb_5 , *Nat. Phys.* **18**, 265 (2022).
- [14] Y. Hu, X. Wu, B. R. Ortiz, S. Ju, X. Han, J. Ma, N. C. Plumb, M. Radovic, R. Thomale, S. D. Wilson, A. P. Schnyder, and M. Shi, Rich nature of van Hove singularities in kagome superconductor CsV_3Sb_5 , *Nat. Commun.* **13**, 2220 (2022).
- [15] M. Kang, S. Fang, J.-K. Kim, B. R. Ortiz, S. H. Ryu, J. Kim, J. Yoo, G. Sangiovanni, D. Di Sante, B.-G. Park, C. Jozwiak, A. Bostwick, E. Rotenberg, E. Kaxiras, S. D. Wilson, J.-H. Park, and R. Comin, Twofold van Hove singularity and origin of charge order in topological kagome superconductor CsV_3Sb_5 , *Nat. Phys.* **18**, 301 (2022).
- [16] Z. Liang, X. Hou, F. Zhang, W. Ma, P. Wu, Z. Zhang, F. Yu, J.-J. Ying, K. Jiang, L. Shan, Z. Wang, and X. H. Chen, Three-dimensional charge density wave and surface-dependent vortex-core states in a kagome superconductor CsV_3Sb_5 , *Phys. Rev. X* **11**, 031026 (2021).
- [17] H. Chen *et al.*, Roton pair density wave in a strong-coupling kagome superconductor, *Nature (London)* **599**, 222 (2021).
- [18] H.-S. Xu, Y.-J. Yan, R. Yin, W. Xia, S. Fang, Z. Chen, Y. Li, W. Yang, Y. Guo, and D.-L. Feng, Multiband superconductivity with sign-preserving order parameter in kagome superconductor CsV_3Sb_5 , *Phys. Rev. Lett.* **127**, 187004 (2021).
- [19] K. Y. Chen, N. N. Wang, Q. W. Yin, Y. H. Gu, K. Jiang, Z. J. Tu, C. S. Gong, Y. Uwatoko, J. P. Sun, H. C. Lei, J. P. Hu, and J.-G. Cheng, Double superconducting dome and triple enhancement of T_c in the kagome superconductor CsV_3Sb_5 under high pressure, *Phys. Rev. Lett.* **126**, 247001 (2021).
- [20] J. Ge, P. Wang, Y. Xing, Q. Yin, A. Wang, J. Shen, H. Lei, Z. Wang, and J. Wang, Evidence for multi-charge flux

- quantization in kagome superconductor ring devices, *Phys. Rev. X* **14**, 021025 (2024).
- [21] B. R. Ortiz, P. M. Sarte, E. M. Kenney, M. J. Graf, S. M. L. Teicher, R. Seshadri, and S. D. Wilson, Superconductivity in the Z_2 kagome metal KV_3Sb_5 , *Phys. Rev. Mater.* **5**, 034801 (2021).
- [22] K. Zhao, H. Lin, X. Xiao, W. Huang, W. Yao, M. Yan, Y. Xing, Q. Zhang, Z.-X. Li, S. Hoshino, J. Wang, S. Zhou, L. Gu, M. Bahramy, H. Yao, N. Nagaosa, Q.-K. Xue, K. Law, X. Chen, and S.-H. Ji, Disorder-induced multifractal superconductivity in monolayer niobium dichalcogenides, *Nat. Phys.* **15**, 904 (2019).
- [23] See Supplemental Material at <http://link.aps.org/supplemental/10.1103/PhysRevMaterials.8.074601> for detail information of an optical image of cleaved KV_3Sb_5 flakes on a sticky tape and the flake thickness measured by scanning electron microscopy.
- [24] B. R. Ortiz, L. C. Gomes, J. R. Morey, M. Winiarski, M. Bordelon, J. S. Mangum, I. W. H. Oswald, J. A. Rodriguez-Rivera, J. R. Neilson, S. D. Wilson, E. Ertekin, M. T. McQueen, and E. S. Toberer, New kagome prototype materials: Discovery of KV_3Sb_5 , RbV_3Sb_5 , and CsV_3Sb_5 , *Phys. Rev. Mater.* **3**, 094407 (2019).
- [25] R. C. Dynes, V. Narayanamurti, and J. P. Garno, Direct measurement of quasiparticle-lifetime broadening in a strongly-coupled superconductor, *Phys. Rev. Lett.* **41**, 1509 (1978).
- [26] X. Wu, T. Schwemmer, T. Müller, A. Consiglio, G. Sangiovanni, D. Di Sante, Y. Iqbal, W. Hanke, A. P. Schnyder, M. M. Denner, M. H. Fischer, T. Neupert, and R. Thomale, Nature of unconventional pairing in the kagome superconductors AV_3Sb_5 ($A = K, Rb, Cs$), *Phys. Rev. Lett.* **127**, 177001 (2021).
- [27] Y. Wang, S.-Y. Yang, P. K. Sivakumar, B. R. Ortiz, S. M. L. Teicher, H. Wu, A. K. Srivastava, C. Garg, D. Liu, S. S. P. Parkin, E. S. Toberer, T. McQueen, S. D. Wilson, and M. N. Ali, Anisotropic proximity-induced superconductivity and edge supercurrent in kagome metal, $K_{1-x}V_3Sb_5$, *Sci. Adv.* **9**, eadg7269 (2023).
- [28] Z. Guguchia *et al.*, Tunable unconventional kagome superconductivity in charge ordered RbV_3Sb_5 and KV_3Sb_5 , *Nat. Commun.* **14**, 153 (2023).
- [29] A. Consiglio, T. Schwemmer, X. Wu, W. Hanke, T. Neupert, R. Thomale, G. Sangiovanni, and D. Di Sante, Van Hove tuning of AV_3Sb_5 kagome metals under pressure and strain, *Phys. Rev. B* **105**, 165146 (2022).